Eur. J. Mineral.
2005, **17**, 143–153

Heulandite-Ba, a new zeolite species from Norway

ALF OLAV LARSEN[1], FRED STEINAR NORDRUM[2], NICOLA DÖBELIN[3], THOMAS ARMBRUSTER[3], OLE V. PETERSEN[4] and MURIEL ERAMBERT[5]

[1]Norsk Hydro ASA, Research Centre Porsgrunn, P. O. Box 2560, N-3907 Porsgrunn, Norway
Corresponding author, e-mail: alf.olav.larsen@hydro.com
[2]Norwegian Mining Museum, P. O. Box 18, N-3602 Kongsberg, Norway
[3]Laboratorium für chemische und mineralogische Kristallographie, University of Bern, Freiestr. 3, CH-3012 Bern, Switzerland
[4]Geological Museum, University of Copenhagen, Øster Voldgade 5–7, DK-1350 Copenhagen, Denmark
[5]Institute for Geology, University of Oslo, P. O. Box 1047 Blindern, N-0316 Oslo, Norway

Abstract: Heulandite-Ba, ideally $(Ba,Ca,Sr,K,Na)_5Al_9Si_{27}O_{72}\cdot 22H_2O$, is a new zeolite species in the heulandite series, occurring as an accessory mineral in hydrothermal veins of the Kongsberg silver deposit type at the Northern Ravnås prospect, southern Vinoren, 14 km NNW of Kongsberg town, Kongsberg ore district, Flesberg community, Buskerud county, Norway. The mineral has also been found at the Bratteskjerpet mine, Saggrenda near Kongsberg, and in hydrothermal veins in quartzite at Sjoa in Sel community, Oppland county. Heulandite-Ba occurs as well developed, thick tabular, trapezoidal crystals up to 4 mm across, showing the forms {100}, {010}, {001}, $\{\bar{1}11\}$ and $\{20\bar{1}\}$. The mineral is colourless to white, rarely very pale yellowish white or pale beige, with a white streak; transparent to translucent, with a vitreous lustre, pearly on {010}. The mineral has a perfect {010} cleavage; subconchoidal to uneven fracture. It is non-fluorescent in long- or short-wave ultraviolet light. The Mohs' hardness is 3½; D_{meas} = 2.35(1) and D_{calc} = 2.350 g/cm^3. Heulandite-Ba is biaxial positive with n_α = 1.5056(5), n_β = 1.5064(5) and n_γ = 1.5150(5); Δ = 0.0094, $n_{(mean)}$ = 1.5090. $2V_\gamma$ (calc) = 34.1°, $2V_\gamma$ (meas) = 38(1)°; distinct dispersion, r > v; $\alpha \wedge$ c varying from ≅ 39° to ≅ 51° in obtuse angle β, γ = b. An average of 14 electron microprobe analyses on heulandite-Ba from the Northern Ravnås prospect, Kongsberg, gave SiO_2 54.26, Al_2O_3 15.27, MgO <0.1, CaO 2.65, SrO 1.03, BaO 12.76, Na_2O 0.34, K_2O 0.58, H_2O 13.1 (from TGA), total 99.99, corresponding to $(Ba_{2.49}Ca_{1.41}Sr_{0.30}K_{0.37}Na_{0.33})_{\Sigma 4.90}Al_{8.96}Si_{27.00}O_{72.00}\cdot 21.75H_2O$ on the basis of 72 framework oxygen atoms. Chemical zoning is frequent, with transitions to heulandite-Ca and heulandite-Sr.

Heulandite-Ba is monoclinic, *C*2/*m*, with *a* = 17.738(3), *b* = 17.856(2), *c* = 7.419(1) Å, β = 116.55(2)°, *V* = 2102.0(7) Å^3, *Z* = 1. The strongest five X-ray diffraction lines of the powder pattern [*d* in Å(*I*)(*hkl*)] are: 2.973(100)(151), 3.978(97)(131), 7.941(66)(200), 4.650(66)(-131), 2.807(65)(–621). The crystal structure refinements (R = 3.5 %) of heulandite-Ba were done in space groups *C*2/*m*, *Cm*, *C*2, and $C\bar{1}$, but refinements in space groups with lower symmetry than *C*2/*m* did not improve the structural model.

Key-words: heulandite-Ba, new mineral, analysis, crystal structure, Norway.

Introduction

Heulandite was first described by Brooke (1822), and has generally been considered as a calcium dominant zeolite. Over the years, however, chemical analyses reveal that other extra-framework cations may be dominant. As a consequence, with the establishment of series among the zeolites, International Mineralogical Association, Commission on New Mineral and Mineral Names, introduced four species among the heulandite series (Coombs *et al*., 1997): heulandite-Ca, heulandite-Sr, heulandite-Na and heulandite-K.

Clinoptilolite is an isostructural zeolite mineral that differs from heulandite for a lower concentration of Al. Coombs *et al*. (1997) suggested to distinguish between heulandite and clinoptilolite on the basis of the Si/Al ratio. Al-rich crystals with Si/Al < 4.0 are heulandites, the less aluminous ones (Si/Al ≥ 4.0) are regarded as clinoptilolites.

Significant amount of barium in heulandite has been reported from a few localities. Lovisato (1897) used the term barium heulandite *(heulandite baritica)* for a barium-bearing heulandite from Sardinia, Italy. The reported chemical analysis showed a content of 2.55 wt.% BaO, and the chemical formula based on his analysis is $(Na_{3.02}Ca_{1.84}Ba_{0.48})_{\Sigma 5.34}Al_{9.46}Si_{27.00}O_{72}\cdot 27.08H_2O$. The mineral is a calcian heulandite-Na, and barium is only a minor component. The name barium heulandite has also been used by Mnatsakanyan *et al*. (1970) for a barium bearing heulandite-Ca with the chemical formula $(Ca_{3.65}Ba_{0.18}Sr_{0.14}Na_{0.99}K_{0.72})_{\Sigma 5.68}$

DOI: 10.1127/0935-1221/2005/0017-0143
0935-1221/05/0017-0143 $ 4.95

$Al_{9.90}Si_{26.37}O_{72}{\cdot}23.85H_2O$, although this mineral has even less Ba than that of Lovisato (1897). Ogawa (1967) reported a heulandite with 4.8 wt.% BaO from Japan. Černý & Povondra (1969) reported a strontian heulandite-Ca with 2.44 wt.% BaO from Czechoslovakia, while Miller & Ghent (1973) described a barian-strontian heulandite-Ca from Alberta, Canada, with a barium content varying from 4.6 to 6.9 wt.% BaO.

During an investigation on minerals of the brewsterite series and their associated minerals in Norway (Larsen *et al*., 2003), the first barium dominant heulandite, heulandite-Ba, was discovered at the Northern Ravnås silver prospect, southern Vinoren, Flesberg community, Buskerud county, Norway. The occurrence is situated 14 km NNW of Kongsberg town, within the Kongsberg ore district. Further investigations revealed that heulandite-Ba also occurred at the Bratteskjerpet silver mine, near Saggrenda 7 km SW of Kongsberg town, and in a road cut at Sjoa, Sel community, Oppland county.

The name heulandite-Ba is in accordance with the nomenclature for new species of previously known zeolite series, using the root name and a suffix including a hyphen and the chemical symbol of the dominant extra-framework cation (Coombs *et al*., 1997). The new mineral species and its name have been approved by the Commission on New Minerals and Mineral Names, International Mineralogical Association (CNMMN no. 2003–001). The holotype specimen of heulandite-Ba from the Northern Ravnås prospect is housed in the collection of Geological Museum, University of Oslo (Catalogue No. 33929).

Heulandite-Ba occurrences

The heulandite-Ba type locality, the Northern Ravnås prospect, is situated within the Kongsberg ore district, which comprises an area of about 30 km in length (in a north – south direction) and 15 km in width. The district is dominated by strongly metamorphosed and tectonized rocks, mainly quartz-plagioclase-biotite gneisses, mica and chlorite schists, amphibolites (metagabbros and metadolerites), and granite gneisses (Bugge, 1917; Starmer, 1985). Roughly parallel to the north – south strike of the rocks are zones (called fahlbands) with disseminated sulphides, predominantly pyrite and pyrrhotite. Age determinations on gneisses have indicated two episodes of metamorphism, about 1600 Ma and 1100–1200 Ma, respectively (Jacobsen & Heier, 1978)

The Precambrian rocks are cut by Permian dolerite dykes, hydrothermal quartz veins and calcite veins deposited along fissures and faults caused by the development of the Oslo Rift (Ihlen, 1986). The silver occurrences are generally found at the intersections between the calcite veins and the fahlbands. The calcite veins normally dip steeply, and most of them have an east – west strike. They measure from a fraction of a millimetre up to about 50 cm in width, and mostly from a few metres to 100 m in length. Brecciation within the veins is common. According to Segalstad (1985 and 2000) the vein minerals were precipitated from hydrothermal solutions at temperatures in the range 200–300 °C and a salinity between 0 and 35 wt.% NaCl-equivalents at depths between 3 and 4 km, with a hydrostatic pressure (from a fluid column) of about 350 atmospheres. Important constituents in the silver bearing calcite veins are quartz, barite, fluorite, native silver, argentite, pyrite, sphalerite, chalcopyrite and coal blende (bitumen), but many other minerals are present in small amounts (Neumann, 1944; Johnsen, 1986 and 1987; Bancroft *et al*., 2001). Many minerals occur in more than one generation.

The Kongsberg Silver Mines were in operation 1623–1958, being historically the largest mining enterprise in Norway. About 300 mines and prospects have been in operation within the Kongsberg ore district (Moen, 1967; Berg, 1998; Helleberg, 2000).

At the Northern Ravnås prospect, heulandite-Ba occurs in calcite-quartz veins of the Kongsberg silver ore type. The veins range from a few mm to 10 cm in thickness. Barite, pyrite, chalcopyrite, sphalerite, galena, silver, acanthite and fluorite are also present. Late stage minerals include zeolites of the brewsterite series, the heulandite series, and harmotome. A late generation calcite usually filled the last empty space in the hydrothermal veins, although small cavities are still quite frequently observed.

The find of barium dominant zeolites at Vinoren promted a re-investigation of previously found heulandites, as well as new search on mine dumps (Nordrum *et al.*, 2003). Subsequently, heulandite-Ba with transition to heulandite-Ca was identified in samples from the dumps of the Bratteskjerpet mine near Saggrenda, in the southern part of the Kongsberg ore district. Also at this locality, the minerals of the heulandite series are associated with minerals of the brewsterite series, harmotome, calcite and minor pyrite.

Strongly zoned crystals composed of heulandite Ba, heulandite-Sr and heulandite-Ca together with quartz, hematite, rutile, anatase, chlorite, albite and minerals of the brewsterite series, were discovered in a sample from a roadcut south of Åmot farm, Sjoa, Sel community, Oppland county, Norway. The mineralization occurs along NE-SW striking, nearly vertical fissures in a metasandstone of late-Precambrian age, metamorphosed during the Caledonian orogeny (Strand, 1951 and 1967; Siedlecka *et al*., 1987). The deposit represents a low-temperature, alpine vein mineralization, and the hydrothermal solutions were probably active during the Caledonian orogeny.

Morphology, physical and optical properties

Heulandite-Ba from the Northern Ravnås prospect occurs as well developed, thick tabular, trapezoidal crystals up to 4 mm across, dominated by the pinacoids {100}, {010} and {001}, modified by $\{\bar{1}11\}$ and $\{20\bar{1}\}$. Aggregates of intergrown crystals up to a few cm across are quite common. Heulandite-Ba from the Bratteskjerpet mine and Sjoa has generally a similar morphology, but the size of the individual crystals is smaller, usually less than 1 mm across. The typical habit of heulandite-Ba crystals is shown in Fig. 1.

Heulandite-Ba is colourless to white, rarely very pale yellowish white or pale beige. The streak is white. It is transparent to translucent with a vitreous lustre, pearly on {010}. The mineral has a perfect {010} cleavage. The fracture is

Table 1. Chemical composition (in oxide weight-%) of minerals of the heulandite series from Northern Ravnås prospect (R1 with compositional ranges in parentheses – R5), Bratteskjerpet mine (B1–B6) and Sjoa (S1–S3), corresponding number of atoms per formula unit based on 72 framework oxygen atoms, and balance error (E %) according to Alietti *et al.* (1977).

	R1		R2	R3	R4	R5	B1	B2	B3	B4	B5	B6	S1	S2	S3
SiO_2	54.26	(52.51-55.91)	53.15	54.20	54.41	55.65	54.51	55.36	54.96	54.96	55.57	55.43	56.54	57.21	53.29
Al_2O_3	15.27	(14.54-15.77)	14.68	14.54	15.35	16.00	16.06	15.46	15.52	15.27	15.64	15.18	17.44	15.65	15.94
MgO	<0.1	(<0.1)	<0.1	<0.1	0.46	<0.1	0.10	0.13	<0.1	<0.1	<0.1	0.20	<0.1	<0.1	<0.1
CaO	2.65	(2.30-2.87)	2.32	2.59	3.40	4.17	2.25	2.93	3.43	3.54	3.85	3.24	4.48	2.82	1.27
SrO	1.03	(0.64-2.18)	0.98	1.55	1.12	5.26	1.75	1.22	2.45	2.72	3.89	1.49	7.90	6.30	2.58
BaO	12.76	(11.17-13.84)	13.84	11.17	9.70	3.20	12.67	11.81	8.00	7.30	5.85	10.22	1.07	5.78	16.57
Na_2O	0.34	(0.23-0.50)	0.41	0.26	0.22	0.76	0.58	0.53	0.67	0.65	0.68	0.59	0.44	0.08	0.39
K_2O	0.58	(0.49-0.86)	0.52	0.53	0.71	0.31	0.68	0.62	0.48	0.51	0.53	0.62	1.20	1.44	0.76
H_2O	13.1														
Total	99.99		85.90	84.84	85.37	85.35	88.60	88.06	85.51	84.95	86.01	86.97	89.07	89.28	90.80
Si	27.008		27.052	27.338	26.943	26.839	26.708	27.000	27.003	27.085	26.950	27.094	26.280	27.095	26.466
Al	8.958		8.806	8.644	8.958	9.094	9.274	8.886	8.987	8.869	8.940	8.745	9.554	8.736	9.330
Mg	0.000				0.340		0.073	0.095				0.146			
Ca	1.413		1.265	1.400	1.804	2.155	1.181	1.531	1.806	1.869	2.001	1.697	2.231	1.431	0.676
Sr	0.297		0.289	0.453	0.322	1.471	0.497	0.345	0.698	0.777	1.094	0.422	2.129	1.730	0.743
Ba	2.489		2.760	2.208	1.882	0.605	2.433	2.257	1.540	1.410	1.112	1.958	0.195	1.073	3.225
Na	0.328		0.405	0.254	0.211	0.711	0.551	0.501	0.638	0.621	0.639	0.559	0.397	0.073	0.376
K	0.368		0.338	0.341	0.449	0.191	0.425	0.386	0.301	0.321	0.328	0.387	0.712	0.870	0.482
H_2O	21.747														
E (%)	-1.50		-6.05	-0.84	-4.25	-2.88	-0.75	-4.88	-0.44	-2.04	-4.68	-6.89	-6.51	-7.17	-8.04

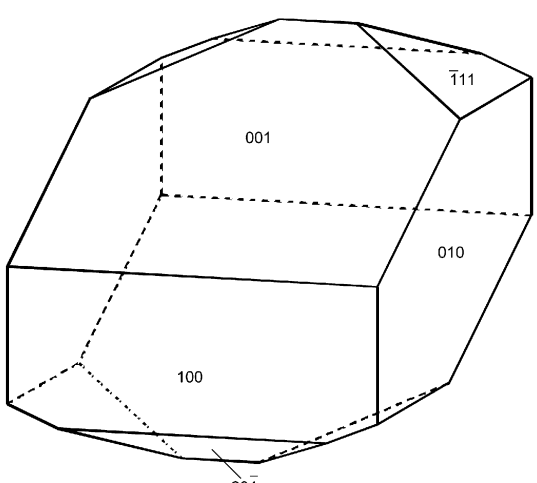

Fig. 1. Drawing of a heulandite-Ba crystal from the Northern Ravnås prospect.

subconchoidal to uneven. No fluorescence in long- or short-wave ultraviolet light was observed. The Mohs' hardness is 3½. The measured density, determined by the sink/float method using di-iodomethane diluted with acetone, is 2.35(1) g/cm^3. The same value, 2.350 g/cm^3, is calculated from the empirical formula, refined cell dimensions (based on XRD powder data), and $Z = 1$. Finely ground heulandite-Ba easily decomposes in warm 6M HCl, leaving silica as a powder. The mineral is rather resistant to cold, diluted acid.

Heulandite-Ba is biaxial positive. The following refractive indices for $\lambda = 589$ nm were determined by means of the microrefractometer spindle-stage, using calcite as refractometer crystal (Medenbach, 1985) and under the application of the λ – T variation method to be: $n_\alpha = 1.5056(5)$, $n_\beta = 1.5064(5)$ and $n_\gamma = 1.5150(5)$; $\Delta = 0.0094$, $n_{(mean)} = 1.5090$. $2V_\gamma$ calculated = 34.1°, $2V_\gamma$ measured directly on the spindle stage = 38(1)°. Heulandite-Ba shows a distinct dispersion, r > v. Both the refractive indices and $2V_\gamma$ are in good agreement with the values given for ordinary heulandite (heulandite-Ca) and in particular with those given for strontian heulandite (Černý & Povonda, 1969; Lucchetti *et al.*, 1982). According to Palmer & Gunter (2000), as well as previous authors, the mean refractive index of natural divalent-exchanged heulandite series zeolites increases with increasing atomic number, and the refractive index parallel to b*, in casu* γ, increases at a greater rate than the refractive indices in (010). The refractive indices of heulandite-Ba confirm their results. The refractive indices of heulandite-Ba also confirm the results of Boles (1972) that samples with Si/Al ratio ≤ 3.5 corresponds to the highest values of the mean refractive indices of heulandite series minerals.

Heulandite-Ba has $\alpha \wedge c$ varying from $\cong 39°$ to $\cong 51°$ in obtuse angle β, $\gamma = b$. The optical orientation for original heulandite (heulandite-Ca) given in most literature, $\alpha \wedge a = 0 – 34°$ and $\beta \wedge c = 0 – 32°$ (see for instance Tröger, 1982) refers to an orthorhombic pseudocell with $\beta \cong 91½°$. When referred to the monoclinic cell, currently accepted for original heulandite (heulandite-Ca), this corresponds to $\alpha \wedge c = 0$ to 34° in obtuse angle β, and $\beta \wedge a = 26½°$ in obtuse angle β to 7½ ° in acute angle β. The optical orientation of heulandite-Ba thus corresponds well with that of ordinary heulandite (heulandite-Ca), and in particular with the optical orientation given by Černý & Provodra (1969) for the predominant part of strontian heulandite crystals studied, disregarding some extreme values they obtained in a limited rim zone of one growth sector.

Heulandite-Ba shows complicated sector zoning with ti-

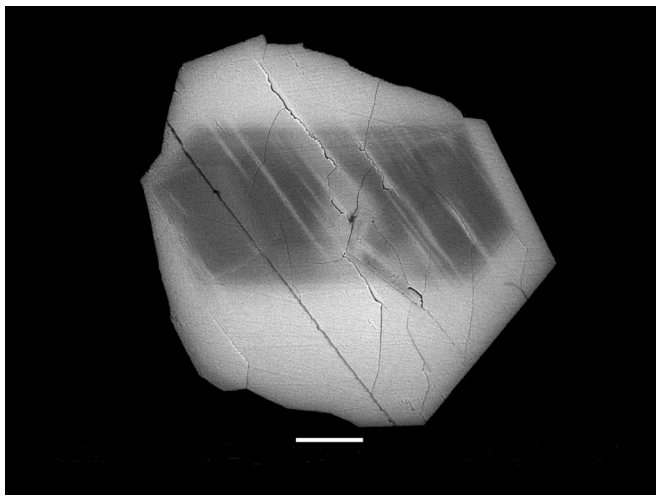

Fig. 2. Backscatter image of a heulandite crystal from Sjoa. Darker areas are enriched in Ca and Sr, while lighter areas are enriched in Ba. Scale bar is 0.1 mm.

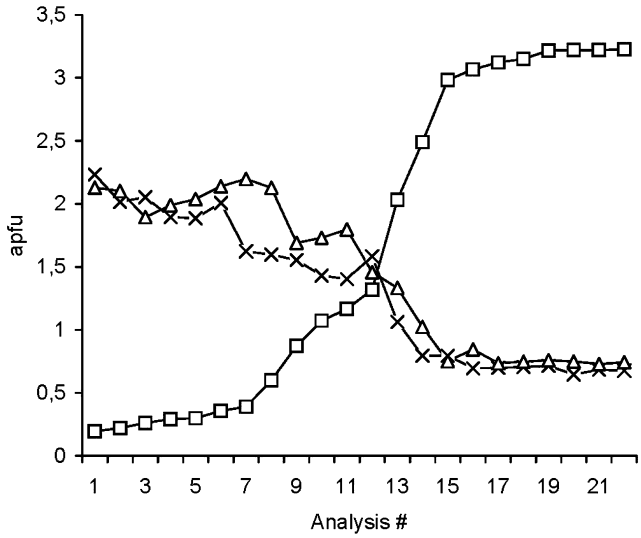

Fig. 3. Variation in divalent cation content in heulandite from Sjoa; Ba (squares), Sr (triangles) and Ca (crosses).

ny differences in refractive indices between some of the zones; twinning has been observed in a few cases.

A Gladstone-Dale calculation gives a compatibility index of 0.011, which is regarded as superior (Mandarino, 1981).

Chemical composition

Chemical analyses of heulandites were carried out by means of a CAMECA SX-100 electron microprobe, operating in wavelength-dispersive mode. The operating conditions were as follows: operating voltage 15 kV, beam current 5 nA, and a beam diameter of 20 µm. The following standards were used: wollastonite (Si$K\alpha$, Ca$K\alpha$), Al_2O_3(Al$K\alpha$), MgO (Mg$K\alpha$), Sr-silicate glass (Sr$L\alpha$), $BaSO_4$ (Ba$L\alpha$) albite (Na$K\alpha$) and orthoclase (K$K\alpha$). Count times for all elements were 10 seconds, exept for K (20 seconds). The water content is derived from the thermogravimetric analysis. The analytical results are given in Table 1.

Backscatter images show that heulandite from the Northern Ravnås prospect is compositionally heterogeneous with an irregular patchy or mottled structure. The mean chemical composition (14 analysis points) of the dominating part of the heulandite-Ba crystal individuals corresponds to the formula (based on 72 framework oxygen atoms) $(Ba_{2.49}Ca_{1.41}Sr_{0.30}K_{0.37}Na_{0.33})_{\Sigma 4.90}Al_{8.96}Si_{27.00}O_{72.00}\cdot 21.75H_2O$ (Table 1, analysis R1), with a compositional range (anhydrous) varying from $(Ba_{2.76}Ca_{1.26}Sr_{0.29}Na_{0.40}K_{0.34})_{\Sigma 5.05}Al_{8.81}Si_{27.05}O_{72.00}$ to $(Ba_{2.20}Ca_{1.40}Sr_{0.45}K_{0.34}Na_{0.25})_{\Sigma 4.64}Al_{8.64}Si_{27.34}O_{72.00}$ (Table 1, analyses R2 and R3). Minor parts of the crystals are depleted in barium, with typical chemical composition $(Ba_{1.88}Ca_{1.80}Mg_{0.34}Sr_{0.32}K_{0.45}Na_{0.21})_{\Sigma 5.00}Al_{8.96}Si_{26.94}O_{72.00}$ (Table 1, analysis R4). A relatively small part, which make up the crystal core, is actually a strontian barian heulandite-Ca with chemical composition $(Ca_{2.15}Sr_{1.47}Ba_{0.60}Na_{0.71}K_{0.19})_{\Sigma 5.12}Al_{9.09}Si_{26.84}O_{72.00}$ (Table 1, analysis R5).

Heulandite from the Bratteskjerpet mine is chemically heterogeneous, shown by backscatter images as a mottled and patchy structure, and with a discrete outer rim in the crystals. The mineral consists of calcian heulandite-Ba interwoven with barian strontian heulandite-Ca (Table 1, analyses B1–B5). The rim is a calcian heulandite-Ba (Table 1, analysis B6).

Backscatter images of heulandite from Sjoa show that the crystals are strongly zoned, and often showing oscillatory crystallization (Fig. 2). The inner part of the crystals is strontian heulandite-Ca (Table 1, analysis S1). Discrete zones outwards are composed of calcian heulandite-Sr of varied composition (represented by analysis S2 in Table 1). The outer part of the crystals, with relatively sharp boundary against the inner part, is heulandite-Ba (Table 1, analysis S3). This is the most barium rich member of the heulandite series ever observed (16.57 wt.% BaO). A compilation of 22 analysis points, showing the variation in composition among the extra-framework divalent cations, is given in Fig. 3. The levels of concentration of Ca and Sr display an inverse correlation towards Ba, and clearly demonstrate the complete solid solution of these elements in heulandite.

The reliability of the zeolite compositions is demonstrated by the balance errors E which are < 10% for all the analysed heulandites (Alietti *et al*., 1977).

The thermogravimetric analysis of heulandite-Ba from the Northern Ravnås prospect was done using a Mettler TG50 instrument linked to a Mettler M3 microbalance. Nitrogen was used as a purge gas, with a flow rate of 100 mL/min. Finely ground sample (7.3650 mg) was heated from 35 °C to 1000 °C at a heating rate of 40 °C per minute. The thermogravimetric curve is shown in Fig. 4. Weight loss occurred in three steps: 1) 35–250 °C, 8.2 wt.% loss, corresponding to 13.6 H_2O, 2) 250–520 °C, 3.4 wt.% loss, corresponding to 5.6 H_2O, and 3) 520–815 °C, 1.5 wt.% loss, corresponding to 2.5 H_2O. A total of 13.1 wt.% loss occurred between 35 °C and 1000 °C, and this value is assumed as the total amount of water in heulandite-Ba. Above 900 °C there was a minor, but gradual loss of weight, probably due to evaporation of alkali. The trippel-stage decomposition of

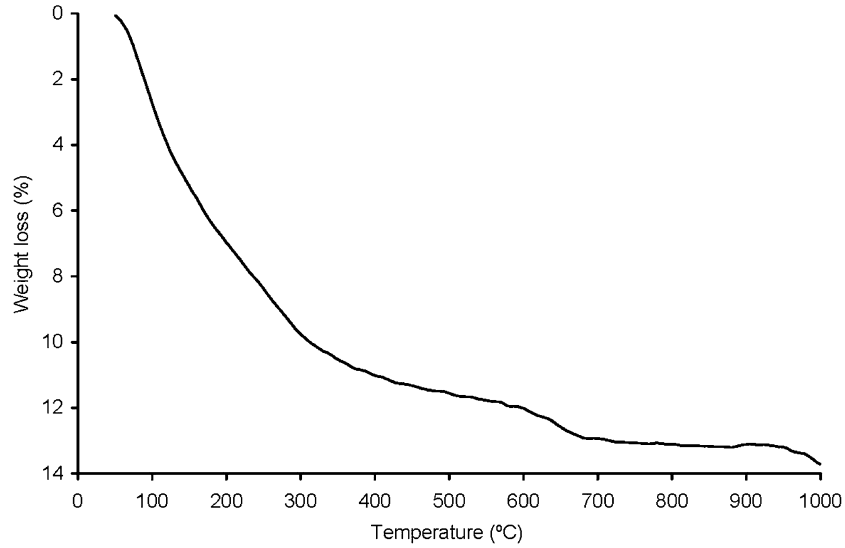

Fig. 4. Thermogravimetric curve of heulandite-Ba.

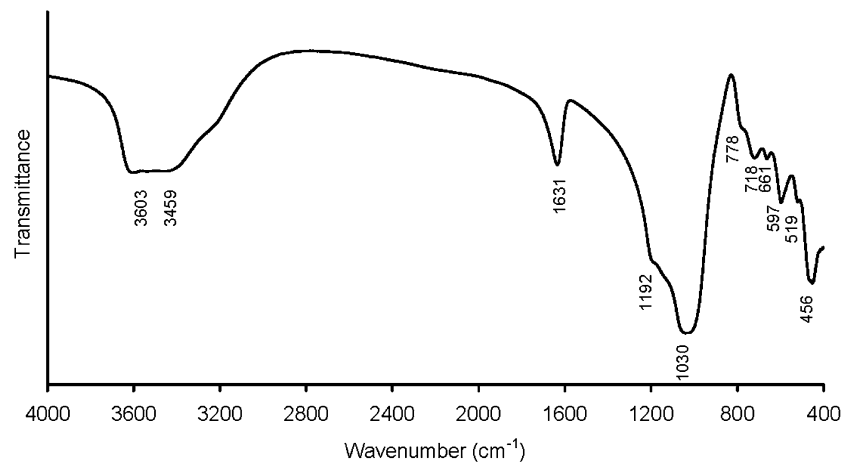

Fig. 5. Infrared spectrum of heulandite-Ba.

heulandite-Ba, caused by differences in water bonding, is typical to that of many heulandites (Gottardi & Galli, 1985).

Heulandite-Ba from the Northern Ravnås prospect was handpicked under a binocular microscope. The material was treated with diluted hydrochloric acid in order to remove traces of calcite. Carefully washed and air dried material was ground, pressed into a KBr pellet, and the infrared spectrum was recorded over the region 400–4000 cm^{-1} using a Perkin Elmer S-2000 FT-IR spectrometer (Fig. 5). The spectrum shows broad absorption bands at 3603 cm^{-1} and 3459 cm^{-1} (O-H stretching), and a sharp absorption band at 1631 cm^{-1} (H-O-H bending). Bands due to absorption by tetrahedral bonds appear at (cm^{-1}, w – weak, m – medium. s – strong, b – broad) 1192 w, 1030 sb, 778 w, 718 m, 661 w, 597 m, 519 w and 456 m.

X-ray crystallography and crystal structure determination

Experimental procedures and results

X-ray powder diffraction data on heulandite-Ba from the Northern Ravnås prospect were obtained using a Philips X'pert diffractometer equipped with automatic divergence slits and diffracted-beam graphite monochromator ($CuK\alpha_1$ radiation, $\lambda = 1.54056$ Å). Data were collected from 3° to 70° 2θ in steps of 0.01° 2θ and 5 s counting time per step. Si (NBS 640a) was used for calibration of the diffractometer. The X-ray powder diffraction data is shown in Table 2. Indexing and least squares refinement were done by the program CELREF (Laugier & Bochu, 1999). The unit cell dimensions found are $a = 17.762(3)$ Å, $b = 17.904(2)$ Å, $c = 7.422(1)$ Å, $\beta = 116.49(1)°$, and $V = 2112.5$ $Å^3$, which is slightly different from the unit cell dimensions found by the crystal structure refinement: $a = 17.738(3)$ Å, $b = 17.856(2)$ Å, $c = 7.419(1)$ Å, $\beta = 116.55(2)°$, and $V = 2102.0$ $Å^3$. The differences are probably due to variations in chemical composition among the material used for the investigations. Calculation of a powder diffraction pattern using the program POWDERCELL (Kraus & Nolze, 1996) shows that heulandite-Ba has ~130 lines with intensity >1 in the region 5–70° 2θ, most of them above 35° 2θ. Obtaining a high quality X-ray powder pattern by a conventional Bragg-Brentano diffractometer is therefore problematic because of insufficient resolution. The pow-

Table 2. X-ray powder diffraction data for heulandite-Ba.

I	*d* (obs.)	*d* (calc.)	*h*	*k*	*l*
26	8.946	8.952	0	2	0
66	7.941	7.948	2	0	0
10	6.846	6.853	-1	1	1
7	6.640	6.643	0	0	1
24	5.942	5.944	2	2	0
5	5.414	5.417	-2	2	1
17	5.266	5.267	-3	1	1
59	5.116	5.117	1	1	1
28	5.085	5.081	3	1	0
66	4.650	4.650	-1	3	1
10	4.480	4.476	0	4	0
26	4.378	4.377	-4	0	1
97	3.978	3.980	1	3	1
16	3.904	3.900	2	4	0
14	3.838	3.839	2	2	1
18	3.738	3.739	-2	4	1
18	3.711	3.712	0	4	1
5	3.633	3.632	4	2	0
48	3.564	3.565	-3	1	2
17	3.484	3.482	-5	1	1
42	3.428	3.427	-2	2	2
22	3.403	3.402	-4	0	2
17	3.323	3.321	0	0	2
56	3.181	3.180	-4	2	2
45	3.131	3.130	5	1	0
24	3.074	3.075	-1	3	2
26	3.038	3.040	-5	1	2
25	2.994	2.992	3	3	1
100	2.973	2.974	1	5	1
6	2.890	2.890	4	0	1
4	2.856	2.856	-2	4	2
65	2.807	2.807	-6	2	1
29	2.734	2.733	-2	6	1
10	2.667	2.667	0	4	2
7	2.636	2.633	-6	2	2
7	2.557	2.559	2	2	2
5	2.539	2.541	6	2	0
5	2.523	2.525	1	7	0
6	2.495	2.496	-7	1	1
6	2.488	2.487	3	5	1
10	2.465	2.466	-4	6	1
7	2.442	2.442	2	6	1
18	2.429	2.430	-7	1	2
5	2.383	2.386	4	6	0
6	2.368	2.368	-4	2	3
10	2.348	2.347	-2	2	3
4	2.325	2.325	-2	6	2
6	2.309	2.307	1	7	1
6	2.301	2.303	3	7	0
5	2.293	2.293	2	4	2
6	2.284	2.284	-3	3	3
7	2.242	2.244	-4	6	2
6	2.236	2.238	0	8	0
3	2.210	2.208	3	3	2
4	2.199	2.199	-6	2	3
6	2.154	2.154	2	8	0
2	2.137	2.137	-2	4	3
8	2.124	2.125	4	0	2
5	2.116	2.115	-7	1	3
16	2.093	2.093	6	2	1
4	2.077	2.076	4	6	1
6	2.058	2.057	1	1	3
11	2.024	2.024	-6	6	2
6	1.968	1.968	-8	4	1
9	1.959	1.959	-1	5	3
8	1.939	1.940	8	2	0
8	1.923	1.923	2	0	3
5	1.873	1.871	-3	9	1
4	1.854	1.855	-4	0	4
2	1.839	1.839	-5	1	4
6	1.829	1.830	-7	5	3
5	1.819	1.819	5	3	2
7	1.791	1.790	0	10	0
9	1.776	1.777	5	7	1
13	1.770	1.770	-7	7	2
5	1.729	1.729	6	0	2
8	1.700	1.699	-10	0	3
7	1.672	1.672	-5	9	2
4	1.654	1.654	-4	8	3
7	1.617	1.616	2	6	3
6	1.594	1.594	3	5	3
5	1.565	1.565	10	2	0
4	1.553	1.553	-6	6	4
5	1.523	1.523	7	3	2
7	1.495	1.495	9	3	1
5	1.486	1.486	-3	11	2
5	1.459	1.458	2	8	3
4	1.454	1.454	-7	9	3
5	1.439	1.439	-5	11	2
6	1.417	1.417	-2	0	5
3	1.400	1.400	-2	8	4
3	1.393	1.393	10	2	1
3	1.388	1.387	-12	4	3
6	1.371	1.371	-9	7	4
8	1.358	1.357	-7	5	5
4	1.345	1.346	-10	2	5

der diffraction pattern in Table 2 reports only well discernible lines.

The crystal structure of heulandite-Ba from the Northern Ravnås prospect was studied by single-crystal X-ray diffraction on an Enraf-Nonius CAD4 diffractometer with graphite-monochromated Mo$K\alpha$ radiation at 293 K. Data reduction, including background and Lorentz-polarization corrections and an empirical absorption correction based on ψ-scans, was performed using the Enraf Nonius SDP program library (Enraf Nonius, 1983). The structure was refined on F^2 by least squares method using the program SHELXTL (Sheldrick, 1997) in space group $C2/m$ and the subgroups $C2$, Cm, and $C\overline{1}$. Refinements in space groups of lower symmetry, however, did not improve the accuracy of the structure model. Refinement in $C2/m$ yielded an $R1$ value of 3.5 %. Detailed information on the data collection and structure refinement are summarized in Table 3. In the following description tetrahedral cation sites (Si, Al) are labelled with *T*, framework oxygens with *O*, extra-framework cations with the appropriate chemical symbol (*Ba*, *Ca*, *Na*, *K*), and oxygen atoms of extra-framework H_2O molecules with *W*.

Table 3. Experimental details of the crystal structure refinement of heulandite-Ba.

Crystal size (mm)	0.300 × 0.125 × 0.250
Composition refined by X-ray data	$(Ba_{2.20}Ca_{1.57}K_{1.61}Na_{0.21})_{\Sigma 5.59}(Al,Si)_{36}O_{72}$ ·20.75H_2O
Composition by EMP (average)	$(Ba_{2.49}Ca_{1.41}Sr_{0.30}K_{0.37}Na_{0.33})_{\Sigma 4.90}Al_{8.96}$ $Si_{27.00}O_{72.00}$·21.75H_2O
Space group	*C*2/*m*
a (Å)	17.738(3)
b (Å)	17.856(2)
c (Å)	7.419(1)
β (°)	116.55(2)
V (Å^3)	2102.0(7)
θ max (°)	29.975
hkl (min., max.)	-24 ≤ h ≤ 23, -25 ≤ k ≤ 25, -1 ≤ l ≤ 10
Scan type	1.5° ω + 0.35 · tan Θ
Measured reflections	7423
Unique reflections	3165
R_{int} (%)	1.83
Obs. reflections (I> 2σ(I))	2731
*R*1 (%)	3.54
*wR*2 (%)	9.76
GooF	1.195

Table 4. Final atomic positional parameters and B_{eq} values (standard deviations in parentheses) for heulandite-Ba.

Atom	sof	x/*a*	y/*b*	z/*c*	B_{eq} (Å^2)
T1	1	0.17934(4)	0.16850(4)	0.09567(9)	1.070(9)
T2	1	0.28857(4)	0.08986(3)	0.50023(9)	1.088(9)
T3	1	0.29214(4)	0.30922(4)	0.28287(9)	1.092(9)
T4	1	0.43568(4)	0.20123(3)	0.58874(9)	1.079(9)
T5	1	0	0.21324(5)	0	1.13(1)
O1	1	0.3047(2)	0	0.5494(4)	2.46(5)
O2	1	0.2684(1)	0.3798(1)	0.3889(3)	2.39(3)
O3	1	0.3171(1)	0.3492(1)	0.1177(3)	2.06(3)
O4	1	0.2385(1)	0.1047(1)	0.2545(3)	2.11(3)
O5	1	0.5	0.1733(2)	0.5	2.45(5)
O6	1	0.0821(1)	0.1586(1)	0.0636(3)	1.83(3)
O7	1	0.3745(2)	0.2660(1)	0.4498(3)	3.09(4)
O8	1	0.0086(1)	0.2677(1)	0.1850(3)	2.50(3)
O9	1	0.2115(1)	0.2531(1)	0.1753(3)	2.13(3)
O10	1	0.3839(1)	0.1275(1)	0.5997(3)	2.25(3)
Ba1	0.359(2)	0.35504(5)	0.5	0.3237(1)	2.48(1)
Ba2	0.190(6)	0.2528(3)	0.5	0.0768(7)	2.67(6)
Ca	0.392(8)	0.4584(1)	0	0.8014(6)	2.20(4)
K	0.41(2)	0.219(1)	0.5	-0.013(3)	5.9(2)
Na	0.05(1)	0.463(2)	0	0.725(9)	1.9(9)*
W1	0.75(2)	0.5774(3)	0.0816(2)	0.9728(7)	3.91(8)
W2	0.36(2)	0.405(2)	0.5	0.155(4)	15(2)*
W3	1	0.5	0	0.5	7.5(2)
W4	0.641(2)	0.425(1)	0.5	0.091(4)	8.4(4)
W5	0.5	0.4824(6)	0.4051(4)	0.507(4)	7.6(2)
W6	0.72(2)	0.4074(6)	0.5	0.719(2)	9.2(3)
W7	0.25(2)	0.605(1)	0.091(1)	0.922(3)	6.0(5)*
W8	0.15(1)	0.385(2)	0.5	0.481(5)	4.74*

Starred atoms were refined isotropically. Anisotropically refined atoms are given in the form of the isotropic equivalent thermal parameter defined as $B_{eq} = 8/3\ \pi^2\ \Sigma_i(\Sigma_j(U_{ij}\ a_i^*\ a_j^*\ a_i\ a_j))$.

The refined chemical composition $(Ba_{2.20}Ca_{1.57}K_{1.61}Na_{0.21})_{\Sigma 5.59}(Al,Si)_{36}O_{72}$·21.15$H_2O$ approximately agrees with the results of the chemical analysis, but in contrast to the electron microprobe analysis no Sr was found. Instead higher populations of the Ca, and in particular K sites, were refined, which is probably caused by partial, but highly disordered, presence of Sr on the same sites. The sum of electrons of the extra-framework sites (XRD: 187.5 e$^-$ pfu, EMPA: 189.7 e$^-$ pfu), however, is almost identical, and thus XRD and EMP experiments are in good agreement.

Extra-framework cations were distinguished from H_2O molecules on the basis of small atomic displacement parameters, as well as appropriate bonding distances to framework oxygens. From various studies describing the cation distribution in natural heulandite/clinoptilolite (Armbruster & Gunter, 2001), we know that the preferred location of a cation in the pore system depends on its ionic radius, therefore the A channel generally contains a Na site (ionic radius 1.16 Å in octahedral coordination) close to the channel wall. This site often also contains Ca (ionic radius 1.14 Å). The Ca site in the B channel is usually Na free, and a K site is located close to the intersection of the A and the C channel. This information, as well as the similarity of the ionic radii of K and Ba, led us to the assumption of a preferred accumulation of Ba in the centre of the C ring, and served as an initial model for the extra-framework cation arrangement.

The tetrahedral framework

The tetrahedral framework of heulandite-Ba shows the common HEU topology forming a two-dimensional system of connected cavities, which leads to three types of structural channels: (i) a ten-membered A channel parallel to the *c* axis, (ii) an eight-membered B channel parallel to the *c* axis, (iii) eight-membered C channels parallel to the *a* axis and [102]. The structure of heulandite-Ba was refined in the monoclinic space group *C*2/*m*, and the data set shows an acceptable quality compared to heulandite structure refinements by Yang & Armbruster (1996) and Stolz & Armbruster (2000). Atom coordinates, occupancies, and B_{eq} values, as well as anisotropic displacement parameters are listed in Table 4 and Table 5, respectively.

For this study, the comparison of our natural heulandite-Ba with the structure refinement of a Ba-exchanged clinoptilolite performed by Petrov *et al*. (1985) is of particular interest. The Ba content in the exchanged sample is 2.54 Ba atoms per formula unit (pfu) normalized to 72 O, and 2.49 Ba atoms pfu in our natural sample. Although the cell dimensions of our sample deviate slightly from both the original and exchanged material reported by Petrov *et al*. (1985), the cell volumes coincide within two standard deviations.

To identify T-sites with high Al concentration we use the average bond length in tetrahedra from central cation to ligands (Si-O = 1.61 Å, Al-O = 1.75 Å) (Kunz & Armbruster, 1990; Alberti & Gottardi, 1988). As shown in Table 6, T2 has the highest Al concentration, while T4 has almost ideal Si-O distances. Therefore it is to be expected that extra-

Table 5. Anisotropic atomic displacement parameters (standard deviations in parentheses) for heulandite-Ba.

Atom	U_{11}	U_{22}	U_{33}	U_{12}	U_{13}	U_{23}
T1	0.0112(3)	0.0171(3)	0.0122(3)	-0.0007(2)	0.0051(2)	0.0007(2)
T2	0.0152(3)	0.0120(3)	0.0143(3)	0.0001(2)	0.0069(2)	0.0001(2)
T3	0.0146(3)	0.0152(3)	0.0124(3)	0.0006(2)	0.0066(2)	0.0006(2)
T4	0.0120(3)	0.0163(3)	0.0121(3)	-0.0006(2)	0.0049(2)	0.0003(2)
T5	0.0117(3)	0.0179(4)	0.0124(4)	0	0.0045(3)	0
O1	0.041(2)	0.015(1)	0.027(1)	0	0.006(1)	0
O2	0.032(1)	0.034(1)	0.033(1)	-0.0030(8)	0.0212(9)	-0.0094(8)
O3	0.035(1)	0.030(1)	0.0204(8)	-0.0051(8)	0.0182(8)	-0.0017(7)
O4	0.0275(9)	0.029(1)	0.0191(8)	0.0087(8)	0.0068(7)	0.0044(7)
O5	0.035(1)	0.034(2)	0.038(2)	0	0.028(1)	0
O6	0.0153(7)	0.0250(9)	0.0290(9)	0.0004(7)	0.0099(7)	0.0022(7)
O7	0.036(1)	0.037(1)	0.035(1)	0.016(1)	0.0078(9)	0.017(1)
O8	0.0268(9)	0.037(1)	0.0251(9)	0.0000(8)	0.0065(8)	-0.0144(8)
O9	0.0227(9)	0.0248(9)	0.035(1)	-0.0091(7)	0.0147(8)	-0.0090(8)
O10	0.0237(9)	0.027(1)	0.033(1)	-0.0082(8)	0.0114(8)	0.0004(8)
Ba1	0.0362(4)	0.0228(3)	0.0351(4)	0	0.0156(3)	0
Ba2	0.041(2)	0.0143(9)	0.057(2)	0	0.031(1)	0
Ca	0.018(1)	0.031(1)	0.028(2)	0	0.0047(8)	0
K	0.065(5)	0.061(3)	0.108(8)	0	0.047(6)	0
W1	0.049(2)	0.050(2)	0.048(2)	0.000(2)	0.020(2)	-0.003(2)
W3	0.098(6)	0.046(4)	0.151(9)	0	0.063(6)	0
W4	0.09(1)	0.072(8)	0.15(1)	0	0.044(9)	0
W5	0.060(8)	0.058(4)	0.134(7)	-0.007(4)	0.01(1)	0.002(6)
W6	0.078(6)	0.15(1)	0.124(9)	0	0.046(6)	0

Table 6. Interatomic bond distances (Å) in Si, Al tetrahedra of heulandite-Ba.

T1 –		T4 –	
O3	1.643(2)	O5	1.629(1)
O4	1.638(2)	O7	1.605(2)
O6	1.641(2)	O8	1.618(2)
O9	1.629(2)	O10	1.628(2)
Mean	1.638(2)	Mean	1.620(2)
T2 –		T5 –	
O1	1.642(1)	O6	1.637(2)
O2	1.654(2)	O6	1.637(2)
O4	1.654(2)	O8	1.633(2)
O10	1.656(2)	O8	1.633(2)
Mean	1.652(2)	Mean	1.635(2)
T3 –			
O2	1.637(2)		
O3	1.641(2)		
O7	1.627(2)		
O9	1.633(2)		
Mean	1.635(2)		

framework cations preferentially bond to T2 ligands to compensate the charge imbalance caused by the substitution of Al^{3+} for Si^{4+}. Armbruster (2001) reported that asymmetric distribution of Al is also reflected in asymmetric distribution of extra-framework cations, and although the Si, Al arrangement is usually not sufficient to influence the symmetry of the HEU framework, asymmetric distribution of extra-framework cations can induce a symmetry lowering (Stolz *et al*., 2000). However, Yang & Armbruster (1996) and Stolz *et al*. (2000) reported that this kind of symmetry lowering can only be detected in homoionic cation exchanged structures. In heulandite-Ba there is no indication of symmetry lowering relative to space group *C*2/*m*.

Distortions of the framework are commonly described by angles between corner sharing tetrahedra. T-O-T connections are stable in the range from approximately 135° to 170° (Gibbs, 1982). At lower angles the repulsive forces between T sites become too strong to form a stable framework. In heulandite-Ba all angles are between 136.0° and 161.9° (Table 7).

The extra-framework sites

The extra-framework cation arrangement is directly related to the Si, Al distribution on tetrahedral sites. As expected from the high Al concentration on T2, three cation sites, Ba1, Ba2, and K, were found near the centre of the C ring (Fig. 6 and 7). All detected cation sites lie on the mirror plane. Ba1, with the highest Ba population of 36 %, bonds to four framework oxygen atoms and is coordinated by the four highly populated H_2O sites W4, W5 (2×), and W6 (Fig. 7, left). At a distance from 1.92 Å to Ba1 a less populated site Ba2 (19 %) is located close to the centre of the C ring as well (Fig. 7, middle). This site bonds to five tetrahedral framework oxygens and is also coordinated by four less populated H_2O sites W4, W7 or W1 (2×), and W8. Bonding distances range from 2.54(2) to 3.08(1) Å for Ba1, and from 2.86(2) to 3.20(2) Å for Ba2, respectively, and thus lie in the acceptable range for Ba-O bond lengths. A third site la-

Table 7. T-O-T angles in heulandite-Ba.

T – O – T angle	(°)
T2 – O1 – T2	155.5(2)
T2 – O2 – T3	146.8(1)
T1 – O3 – T3	140.9(1)
T1 – O4 – T2	139.5(1)
T4 – O5 – T4	144.4(2)
T1 – O6 – T5	136.0(1)
T3 – O7 – T4	161.8(2)
T4 – O8 – T5	149.4(1)
T1 – O9 – T3	146.6(1)
T2 – O10 – T4	142.5(1)

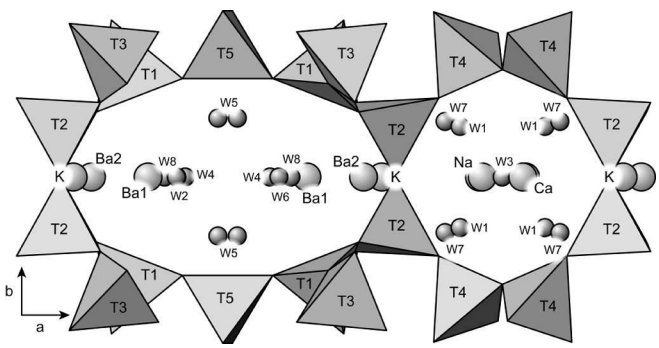

Fig. 6. The A (left) and B (right) channel of heulandite-Ba shown in a polyhedral representation of the HEU structure projected along [001]. Ba1, Ba2, and K are located close to T2, the tetrahedron with the highest Al concentration. Large spheres represent extra-framework cations, small spheres are H_2O molecules.

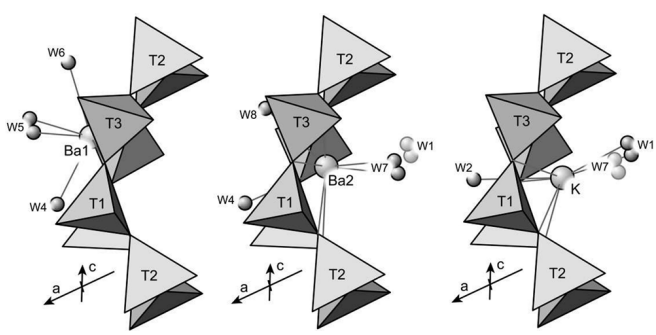

Fig. 7. The three cation site Ba1, Ba2 and K are located near the centre of the C ring, here shown in a projection parallel [101]. Each site bonds to framework oxygens, preferentially to vertice of the Al-rich T2 tetrahedron, and is irregularly coordinated by H_2O molecules.

belled K is also part of the cluster at the intersection of the A and C channel (Fig. 7, right). It contains K, Sr, and minor Ba, and bonds to four framework oxygens and to additional H_2O molecules. Atomic displacement parameters and their standard deviations of this site are significantly higher compared to all other extra-framework cation sites (see Table 5), indicating overlap of different atomic species such as Sr, K, and Ba. This fact was not considered in the structure refinement, instead, the K site was treated as if it was partially occupied by K^+. Since minor Sr and Ba share the site, the refinement results in a too high concentration of K.

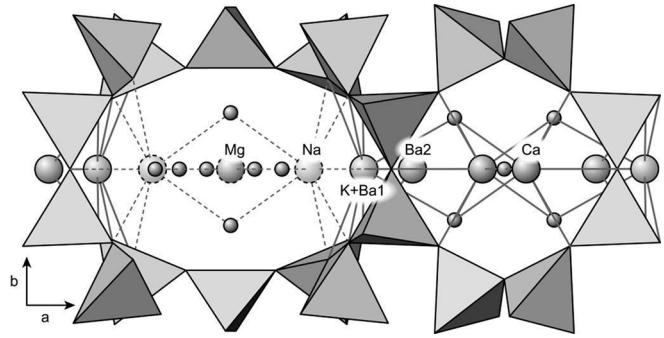

Fig. 8. A polyhedral representation of the structure of Ba-exchanged clinoptilolite described by Petrov *et al*. (1985) is shown in a projection parallel to [001]. Ions drawn in broken lines (Na and Mg) represent sites with occupancies close to the detection limit (symmetric equivalent sites are only labelled once). All Ba is located in a cluster in the C ring (K + Ba1, Ba2). The fact that less H_2O sites were found by Petrov *et al*. can probably be explained by the lower resolution of powder X-ray structure refinements compared to single-crystal X-ray data.

Table 8. Interatomic bond distances (Å) of the extra-framework cation sites in heulandite-Ba.

Ba1 –		Ca –	
W4	2.54(2)	W1 (2x)*	2.407(5)
W5 (2x)	3.08(1)	W1 (2x)	2.507(7)
W6	2.65(1)	W3	2.649(5)
O2 (2x)	2.804(2(	W7 (2x)*	2.85(2)
O3 (2x)	3.020(2)	O1	2.525(4)
		O10 (2x)	2.720(3)
Ba2 –			
W1 (2x)*	3.20(2)	Na –	
W4	3.01(2)	W1 (2x)*	2.50(3)
W7 (2x)*	2.86(2)	W3	2.04(7)
W8	2.86(3)	W7 (2x)*	2.79(3)
O2 (2x)	3.077(4)	O1	2.52(3)
O3 (2x)	2.888(3)	O10 (2x)	2.62(2)
O4	3.147(3)		
K –			
W1 (2x)*	2.867(9)		
W2	2.95(4)		
W4	3.38(2)		
W7 (2x)*	2.48(2)		
O3 (2x)	3.116(9)		
O4 (2x)	2.910(8)		

* Starred bonds do not occur simultaneously.

The cation composition in the B channel agrees with other structure refinements of natural heulandites/clinoptilolites (Armbruster & Gunter, 1991): Two unique sites labelled Ca and Na are occupied by the corresponding elements to 39 % and 5 %, respectively. The distance between the two positions amounts to 0.61 Å, thus neighbouring sites cannot be occupied simultaneously. Although Armbruster & Gunter (2001) reported that Na in the B channel is very uncommon, small amounts are reasonable due to the very similar atomic radii of Na and Ca. Na sites in the B channel are also known

from Na-exchanged heulandites (Yang & Armbruster, 1996). Both Ca and Na form three bonds to framework oxygens and to the partially occupied H_2O sites W1, W7, and W3, the latter being situated on the intersection of the mirror plane and the twofold axis. The distance between the H_2O sites W1 and W7, with occupancies 75 % and 25 %, respectively, amounts to 0.74 Å and again inhibits simultaneous occupancy of both sites. The two sites, however, can be regarded as a fully occupied H_2O site that is split into two parts. A list of interatomic bonding distances of the extra-framework cation sites to the coordinating oxygen atoms is shown in Table 8. The extra-framework sites Na, W2, W7, and W8 were refined isotropically due to their low populations.

Prior to this study, heulandites/clinoptilolites with high Ba concentrations were only known from cation-exchange experiments. The structure of an exchanged clinoptilolite sample with the formula $(Ba_{2.54}Ca_{0.42}Mg_{0.18}K_{0.34}Na_{0.10})_{\Sigma 3.58}(Al_{6.20}Si_{29.62})_{\Sigma 35.82}O_{72}\cdot 19.7H_2O$ was refined from powder X-ray diffraction data and described by Petrov *et al*. (1985) and shown in Fig. 8. Surprisingly, our natural sample has almost the same Ba concentration (2.49 Ba pfu). The cation distribution in the channels is nearly identical: In both samples all Ba is accumulated in the centre of the C ring distributed among three cation sites, one of which is shared by two elements. Our K site (containing K, Sr, and minor Ba) is occupied by Ba in the exchanged sample and located closer to the centre of the B channel. Our Ba2 site is shared by Ba and K, and our Ba1 site contains only minor amounts of Na in the structure described by Petrov *et al*. (1985). The weakly occupied Na site in the B channel is not present in the exchanged sample. Instead a very low-populated Mg site in the centre of the A channel (on the intersection of the twofold axis and the mirror plane) was found. In general, the location of the cation sites of both structures roughly agrees, apart from the very low-populated sites close to the detection limit. Differences are found in the distribution of the elements on the clustered sites in the C ring.

Acknowledgements: We are indebted to P. Berget for providing samples from the Sjoa locality, and H. Kristiansen and B. Jacobsen for providing samples from Vinoren. We thank I. Liberger, A. Henriksen and T. Bach, all at Norsk Hydro ASA, Research Centre Porsgrunn, for carrying out the TG analysis, the IR spectrometric analysis and the SEM images, respectively. Nicola Döbelin and Thomas Armbruster acknowledge support from the Swiss National Science Foundation (Grant 20-65084.01 to TA: crystal chemistry of minerals). We thank A. Alberti, an anonymous referee, associate editor E. Passaglia and chief editor R. Altherr for their comments.

References

Alberti, A. & Gottardi, G. (1988): The determination of the Al-content in the tetrahedra of framework silicates. *Z. Kristallogr.*, **184**, 49-61.

Alietti, A., Brigatti, M.F., Poppi, L. (1977): Natural Ca-rich clinoptilolites (heulandites of group 3): new data and review. *N. Jb. Miner. Mh.*, **1977**, 493-501.

Armbruster, T. (2001): Clinoptilolite-heulandite: applications and basic research. *in* "Studies in surface science and catalysis, 135. Zeolites and mesoporous materials at the dawn of the 21st century", Elsevier Science B. V., 13-27.

Armbruster, T. & Gunter, M.E. (1991): Stepwise dehydration of heulandite-clinoptilolite from Succor Creek, Oregon, U.S.A.: A single-crystal X-ray study at 100 K. *Am. Mineral.*, **76**, 1872-1883.

–, – (2001): Crystal structures of natural zeolites. *in* "Natural zeolites: occurrence, properties, applications", Reviews in mineralogy and geochemistry, vol. **45**, Mineralogical Society of America, 1-67.

Bancroft, P., Nordrum, F.S., Lyckberg, P. (2001): Kongsberg revisited. *Miner. Rec.*, **32**, 181-205.

Berg, B.I. (1998): Gruveteknikk ved Kongsberg Sølvverk 1623–1914. Senter for teknologi og samfunn, report 37, 586 p.

Boles, J.R. (1972): Composition, optical properties, cell dimensions, and thermal stability of some heulandite group zeolites. *Am. Mineral.*, **57**, 1463-1493.

Brooke, H.J. (1822): On the comptonite of Vesuvius, the brewsterite of Scotland, the stilbite and the heulandite. *Edinb. Phil. J.*, **l6**, 112-115.

Bugge, C. (1917): Kongsbergfeltets geologi. *Nor. Geol. Unders.,* **82**, 1-272.

Černý, P. & Povondra, P. (1969): A polycationic, strontian heulandite; comments on crystal chemistry and classification of heulandite and clinoptilolite. *N. Jb. Miner. Mh.*, **1969**, 349-361.

Coombs, D.S., Alberti, A., Armbruster, T., Artioli, G., Colella, C., Galli, E., Grice, J.D., Liebau, F., Mandarino, J.A., Minato, H., Nickel, E.H., Passaglia, E., Peacor, D.R., Quartieri, S., Rinaldi, R., Ross, M., Sheppard, R.A., Tillmanns, E., Vezzalini, G. (1997): Recommended nomenclature for zeolite minerals: Report of the subcommittee on zeolites of the International Mineralogical Association, Commission on New Mineral and Mineral Names. *Can. Mineral.*, **35**, 1571-1606 (also published (1998): *Miner. Mag.*, **62**, 533-571).

Enraf Nonius (1983): Structure determination package (SDP). Enraf Nonius, Delft, The Netherlands.

Gibbs, G.V. (1982): Molecules as models for binding in silicates. *Am. Mineral.,* **67**, 421-450.

Gottardi, G. & Galli, E. (1985): Natural zeolites. Springer-Verlag, Berlin, Heidelberg, New York, Tokyo, 409 p.

Helleberg, O.A. (2000): Kongsberg Sølvverk 1623-1958. Forlaget Langs Lågen, Kongsberg, 374 p.

Ihlen, P.M. (1986): The metallogeny of the Kongsberg district. *Sver. Geol. Unders., Ser. Ca,* **59**, 30-32.

Jacobsen, S.B. & Heier, K.S. (1978): Rb-Sr isotope systematics in metamorphic rocks, Kongsberg sector, south Norway. *Lithos*, **11**, 257-276.

Johnsen, O. (1986): Famous mineral localities: the Kongsberg silver mines, Norway. *Miner. Rec.*, **17**, 19-36.

– (1987): Silber aus Norwegen. Zur Bergbaugeschichte und über die Mineralienschätze. *Emser Hefte*, **8**,1-48.

Kraus, W. & Nolze, G. (1996): POWDER CELL – a program for the representation and manipulation of crystal structures and calculation of the resulting X-ray powder patterns. *J. Appl. Cryst.*, **29**, 301-303.

Kunz, M. & Armbruster, T. (1990): Difference displacement parameters in alkali feldspars – Effects of (Si,Al) order-disorder. *Am. Mineral.*, **75**, 141-149.

Larsen, A.O., Nordrum, F.S., Erambert, M. (2003): Mineraler i brewsterittserien fra norske lokaliteter. *Norsk Bergverksmuseum Skrift*, **25**, 41-42.

Laugier, J. & Bochu, B. (1999): CELREF: Cell parameters refine-

ment program from powder diffraction diagram. Laboratoire des Matériaux et du Génie Physique, Ecole Nationale Supérieure de Physique de Grenoble (INPG), Grenoble, France.

Lovisato, D. (1897): Notizia sopra una heulandite baritica di Pula con acceno alle zeoliti finora trovate in Sardegna. *Atti della Reale Acc. Lincei, Rend., 5. Ser.*, **6**, 260-264.

Lucchetti, G., Massa, B., Penco, A.M. (1982): Strontian heulandite from Campegli (Eastern Ligurian ophiolites, Italy). *N. Jb. Miner. Mh.*, **1982**, 541-550.

Mandarino, J.A. (1981): The Gladstone-Dale relationship: Part IV. The compatibility concept and its application. *Can. Mineral.*, **19**, 441-450.

Medenbach, O. (1985): A new microrefractometer spindle-stage and its application. *Fortschr. Miner.*, **61**, 111-133.

Miller, B.E. & Ghent, E.D. (1973): Laumontite and barian-strontian heulandite from the Blairmore Group (Cretaceous), Alberta. *Can. Mineral.*, **12**, 188-192.

Mnatsakanyan, A.Kh., Khurshudyan, E.Kh., Revazova, N.V. (1970): Zeolites from the Upper Cretaceous volcanic formations in the northeastern part of the Armenian SSR. *Zap. Arm. Otd. Vses. Mineral. Obshchest.,* **4**, 141-160 (in Russian).

Moen, K. (1967): Kongsberg Sølvverk 1623-1957. Universitetsforlaget, Oslo, 482 p.

Neumann, H. (1944): Silver deposits at Kongsberg. *Nor. Geol. Unders.*, **162**, 1-133.

Nordrum, F.S., Larsen, A.O., Erambert, M. (2003): Minerals of the heulandite series in Norway – a progress report. *Norsk Bergverksmuseum Skrift*, **25**, 51-62.

Ogawa, T. (1967): On the varieties of heulandites. *J. Sci. Hiroshima Univ., Ser. C (Geol. Mineral.)*, **5**, 267-286.

Palmer, J.L. & Gunter, M.E. (2000): Optical properties of natural and cation exchanged heulandite group zeolites. *Am. Mineral.*, **85**, 225-230.

Petrov, O.E., Filizova, L.D., Kirov, G.N. (1985): Cation distribution in the clinoptilolite structure: Ba-exchanged sample. *Compt. Rend. l'Acad. Bulg. Sci.*, **38**, 603-606.

Segalstad, T.V. (1985): Sølvdannelsen i Kongsberg sølvforekomst. Ore geology symposium "Nye malmtyper i Norge", Bergverkenes Landssammenslutnings Industrigruppe, Bergforskningen (abstract), 100.

– (2000): Native silver from Kongsberg. *in* "Highlights, selected attractions, Natural History Museums and Botanical Garden" , E. Roaldset, & S.-E. Sjulsen, eds. University of Oslo, 34-39.

Sheldrick, G.M. (1997): SHELX-97: Program for crystal structure refinement. Univ. Göttingen, Germany.

Siedlecka, A., Nystuen, J.P., Englund, J.O., Hossack, J. (1987): Lillehammer, geological map 1:250000. Norges Geologiske Undersøkelse, Trondheim.

Starmer, I.C. (1985): The geology of the Kongsberg district and the evolution of the entire Kongsberg sector, South Norway. *Nor. Geol. Unders., Bull.,* **401**, 35-58.

Stolz, J. & Armbruster, T. (2000): Mg^{2+}, Mn^{2+}, Cd^{2+}, Sr^{2+}, and Cu^{2+} exchange in heulandite single crystals: X-ray structure refinements. *in* "Natural zeolites for the third millennium", C. Colella & F.A. Mumpton, eds. De Frede Editore, Napoli, 119-138.

Stolz, J., Yang, P., Armbruster, T. (2000): Cd-exchanged heulandite: symmetry lowering and site preference. *Microporous and Mesoporous Materials*, **37**, 233-242.

Strand, T. (1951): The Sel and Vågå map areas. *Nor. Geol. Unders.*, **178**, 1-117.

– (1967): Stratigraphy and structure of Eocambrian and younger deposits in a part of the Gudbrandsdal valley district, South Norway. *Nor. Geol. Unders.*, **251**, 93-106.

Tröger, W.E. (1982): Optische Bestimmung der Gesteinsbildenden Minerale, Teil 1 Bestimmungstabellen, 5. neubearbeitete Auflage von H.U. Bambauer, F. Taborszky, H.D. Trochim. E. Schweizerbart'sche Verlagsbuchhandlung (Nägele und Obermiller), Stuttgart, 188 p.

Yang, P. & Armbruster, T. (1996): Na, K, Rb, and Cs exchange in heulandite single- crystals: X-ray structure refinements at 100 K. *J. Solid State Chem.*, **123**, 140-149.

Received 17 November 2003
Modified version received 22 June 2004
Accepted 11 November 2004